PLOS ONE

RESEARCH ARTICLE

Spatial Heterogeneity, Host Movement and Mosquito-Borne Disease Transmission

Miguel A. Acevedo[1]*, Olivia Prosper[2], Kenneth Lopiano[3], Nick Ruktanonchai[4], T. Trevor Caughlin[4], Maia Martcheva[5], Craig W. Osenberg[6], David L. Smith[7]

1 University of Puerto Rico–Río Piedras, Department of Biology, San Juan, PR, USA, **2** Dartmouth College, Department of Mathematics, Hanover, NH, USA, **3** Statistical and Applied Mathematical Sciences Institute, Durham, NC, USA, **4** University of Florida, Department of Biology, Gainesville, FL, USA, **5** University of Florida, Department of Mathematics, Gainesville, FL, USA, **6** University of Georgia, Odum School of Ecology, Athens, GA, USA, **7** Department of Epidemiology and Malaria Research Institute, John Hopkins Bloomberg School of Public Health, Baltimore, MD, USA

* miguel.acevedo7@upr.edu

Citation: Acevedo MA, Prosper O, Lopiano K, Ruktanonchai N, Caughlin TT, Martcheva M, et al. (2015) Spatial Heterogeneity, Host Movement and Mosquito-Borne Disease Transmission. PLoS ONE 10(6): e0127552. doi:10.1371/journal.pone.0127552

Academic Editor: James M McCaw, The University of Melbourne, AUSTRALIA

Received: May 8, 2014

Accepted: April 16, 2015

Published: June 1, 2015

Data Availability Statement: All relevant data are available via Github (https://github.com/maacevedo/Spatial-heterogeneity-host-movement-and-vector-borne-disease-transmission) and within the supporting information files.

Funding: This work was supported by National Science Foundation (NSF) Quantitative Spatial Ecology, Evolution, and Environment (QSE3) Integrative Graduate Education and Research Traineeship Program Grant 0801544, and NSF Doctoral Dissertation Improvement Grant (DEB-1110441). The funders had no role in study design,

Abstract

Mosquito-borne diseases are a global health priority disproportionately affecting low-income populations in tropical and sub-tropical countries. These pathogens live in mosquitoes and hosts that interact in spatially heterogeneous environments where hosts move between regions of varying transmission intensity. Although there is increasing interest in the implications of spatial processes for mosquito-borne disease dynamics, most of our understanding derives from models that assume spatially homogeneous transmission. Spatial variation in contact rates can influence transmission and the risk of epidemics, yet the interaction between spatial heterogeneity and movement of hosts remains relatively unexplored. Here we explore, analytically and through numerical simulations, how human mobility connects spatially heterogeneous mosquito populations, thereby influencing disease persistence (determined by the basic reproduction number R_0), prevalence and their relationship. We show that, when local transmission rates are highly heterogeneous, R_0 declines asymptotically as human mobility increases, but infection prevalence peaks at low to intermediate rates of movement and decreases asymptotically after this peak. Movement can reduce heterogeneity in exposure to mosquito biting. As a result, if biting intensity is high but uneven, infection prevalence increases with mobility despite reductions in R_0. This increase in prevalence decreases with further increase in mobility because individuals do not spend enough time in high transmission patches, hence decreasing the number of new infections and overall prevalence. These results provide a better basis for understanding the interplay between spatial transmission heterogeneity and human mobility, and their combined influence on prevalence and R_0.

data collection and analysis, decision to publish, or preparation of the manuscript.

Competing Interests: The authors have declared that no competing interests exist.

Introduction

More than half of the world's population is infected with some kind of vector-borne pathogen [1–3], resulting in an enormous burden on human health, life, and economies [4]. Vector-borne diseases are most common in tropical and sub-tropical regions; however, their geographic distributions are shifting because of vector control, economic development, urbanization, climate change, land-use change, human mobility, and vector range expansion [5–9].

Mathematical models continue to play an important role in the scientific understanding of vector-borne disease dynamics and informing decisions regarding control [10–14] and elimination [15–17], owing to their ability to summarize complex spatio-temporal dynamics. Although there is increasing interest in the implications of spatial processes for vector-borne disease dynamics [18–22], most models that describe these dynamics assume spatially homogeneous transmission, and do not incorporate host movement [23–25]. Yet, heterogeneous transmission may be the rule in nature [26–28], where spatially heterogeneous transmission may arise due to spatial variation in vector habitat, vector control, temperature, and rainfall, influencing vector reproduction, vector survival and encounters between vectors and hosts [29, 30].

Movement of hosts among patches with different transmission rates links the pathogen transmission dynamics of these regions [31]. In the resulting disease transmission systems some patches may have environmental conditions that promote disease transmission and persistence (*i.e.*, hotspots), while other patches may not be able to sustain the disease without immigration of infectious hosts from hotspots [32]. Control strategies often focus on decreasing vectorial capacity in hotspots [33, 34] with some successes, such as malaria elimination from Puerto Rico [35], and some failures [36, 37], such as malaria control efforts in Burkina Faso [38]. An often overlooked factor when defining sites for control efforts is a patch's connectivity to places of high transmission. For example, malaria cases during the 1998 outbreak in the city Pochutla, Mexico were likely caused by human movement into the city from nearby high transmission rural areas, despite active vector control in Pochutla [39]. Understanding the interaction between connectivity—defined by the rate of movement of hosts among patches—and spatial heterogeneity in transmission via mathematical models has the potential to better inform control and eradication strategies of mosquito-borne diseases in real-world settings [37, 40].

In this study, we ask, how host movement and spatial variation in transmission intensity influense malaria long-term persistence and prevalence. First, we show analytically that transmission intensity is an increasing function of spatial heterogeneity in a two-patch system, where the patches are connected by host movement. Second, we apply a multi-patch adaptation of the Ross-Macdonald modeling framework for malaria dynamics to explore the implications of spatial heterogeneity in transmission intensity and human movement for disease prevalence and persistence. The mosquitoes that transmit malaria typically move over much smaller spatial scales than their human hosts. Thus, we assume that mosquito populations are isolated in space. The varying size of mosquito populations across a landscape introduces spatial heterogeneity in transmission intensity. This heterogeneity, coupled with the fact that humans commonly move among areas with varying degrees of malaria transmission, makes malaria an ideal case study.

Materials and Methods

The Ross-Macdonald modeling approach describes a set of simplifying assumptions that describe mosquito-borne disease transmission in terms of epidemiological and entomological processes [41]. Although it was originally developed to describe malaria dynamics, the modeling framework is simple enough to have broad applicability to other mosquito-borne

infections. One of the most important contributions of the Ross-Macdonald model is the identification of the threshold parameter for invasion R_0, or the basic reproductive number. Threshold quantities, such as R_0, often form the basis of planning for malaria elimination. In some cases R_0 also determines the long-term persistence of the infection. Here, we define persistence to mean *uniform strong persistence* of the disease; that is whether the disease will remain endemic in the population, and bounded below by some positive value, over the long term. Mathematically, a disease is *uniformly strongly persistent* if there exists some $\epsilon > 0$ such that $\limsup_{t \to \infty} I(t) \geq \epsilon$ for any $I(0) > 0$, where $I(t)$ is the number of infected individuals at time t [42, 43].

To extend the Ross-Macdonald model to a landscape composed of $i = 1, \ldots, Q$ patches we need to account for the rate of immigration and emigration of humans among the Q patches. The full mathematical derivation of the multi-patch extension (Eq 1) from the original Ross-Macdonald model can be found in S1 Text.

For each patch i, the rates of change in the proportion of infected mosquitoes, the number of infected hosts, and the total number of humans are calculated as

$$\begin{aligned}
\frac{dz_i}{dt} &= a_i c_i \frac{I_i}{N_i}(e^{-g_i n_i} - z_i) - g_i z_i \\
\frac{dI_i}{dt} &= m_i a_i b_i z_i (N_i - I_i) - r_i I_i - I_i \sum_{j \neq i}^{Q} k_{ji} + \sum_{j \neq i}^{Q} k_{ij} I_j \\
\frac{dN_i}{dt} &= -N_i \sum_{j \neq i}^{Q} k_{ji} + \sum_{j \neq i}^{Q} k_{ij} N_j
\end{aligned}$$

where N_i describes the total size of the human population in patch i, I_i represents the number of infected hosts in patch i, z_i represents the proportion of infected mosquitoes in patch i, and k_{ji} represents the rate of movement of human hosts from patch i to patch j. Note that $1/k_{ji}$ describes the amount of time (days in this particular parameterization) an individual spends in patch i before moving to patch j. For simplicity, we assumed that the rate of host movement was symmetric between any two patches, and equal amongst all patches, such that $k = k_{ij} = k_{ji}$. We further assumed that the initial human population densities for each patch were equal. This constraint on the initial condition, along with the assumption of symmetric movement, causes the population size of each patch to remain constant, that is, $dN_i/dt = 0$ for all i. We also assumed that the only parameter that varies among patches is the ratio of mosquitoes to humans, m_i. The rate a_i at which mosquitoes bite humans, the probability c_i a mosquito becomes infected given it has bitten an infected human, the probability b_i a susceptible human is infected given an infectious mosquito bite, the mosquito death rate g_i, the human recovery rate r_i, and the extrinsic incubation period (the incubation period for the parasite within the mosquito) n_i, are all assumed constant across the landscape. Consequently, for all $i = 1, \ldots, Q$, $a_i = a$, $b_i = b$, $c_i = c$, $g_i = g$, $r_i = r$, and $n_i = n$.

In this model there is no immunity conferred after infection. Furthermore, although host demography (births and deaths) can play an important role in transient disease dynamics, because our focus is the relationship between equilibrium prevalence and R_0 under the assumption of constant patch population sizes, we omit host demography. Choosing constant birth rates $\Lambda = \mu N$ and natural host mortality rates μ in each patch yields identical R_0 and equilibria to our model, with the exception that r is replaced by $r + \mu$. Thus, including host demography in this way would result in a slight decrease in R_0 and prevalence by decreasing the infectious period. How host demography influences the relationship between R_0 and prevalence when patch population sizes are not constant, and moreover, when host demography is

heterogeneous, is an interesting question that remains to be explored. These simplifying assumptions yield the following system of $2Q$ equations,

$$\begin{aligned} \frac{dz_i}{dt} &= ac\frac{I_i}{N}(e^{-gn} - z_i) - gz_i \\ \frac{dI_i}{dt} &= m_i abz_i(N - I_i) - rI_i - I_i\sum_{j\neq i}^{Q} k + \sum_{j\neq i}^{Q} kI_j \end{aligned} \tag{1}$$

Analyses

Differences in the ratio of mosquitoes to humans, m_i results in a network of heterogeneous transmission, where each patch in the network is characterized by a different transmission intensity. The basic reproduction number for an isolated patch (i.e., one not connected to the network through human movement) is defined by $R_{0,i} = \frac{\alpha_i\beta}{rg}$, where $\alpha_i := m_i\, abe^{-gn}$ and $\beta := ac$, and is a measure of local transmission intensity. Furthermore, $R_{0,i}$ is a threshold quantity determining whether disease will persist in patch i in the absence of connectivity. In particular, if $R_{0,i} > 1$, malaria will persist in patch i, while if $R_{0,i} \leq 1$, it will go extinct in the absence of connectivity with other patches. $R_{0,i}$ (local transmission) increases with the ratio of mosquitoes to humans m_i, and if more transmission occurs, more people are infected at equilibrium. These results, however, do not necessarily hold in a network where hosts move among patches [20]. Indeed, movement can cause the disease to persist in a patch where it would otherwise die out [20, 44].

To address this limitation of the isolated patch reproduction number, we used the next generation approach [45, 46] to calculate R_0 for the whole landscape. This approach requires the construction of a matrix $K = FV^{-1}$, where $J = F - V$ is the Jacobian of the $2Q$-dimensional system evaluated at the disease-free equilibrium, F is nonnegative, and V is a nonsingular M-matrix. F contains terms related to new infection events, and V contains terms of the Jacobian related to either recovery or migration events. This choice satisfies the conditions for the theory to hold, and the important consequence of this approach is that the spectral radius of the next generation matrix $\rho(K)$ is less than one if and only if the disease-free equilibrium is locally asymptotically stable. Defining $R_0 = (\rho(K))^2$, we have that the disease-free equilibrium is locally asymptotically stable when $R_0 < 1$ and unstable when $R_0 > 1$. We proved (see S2 Text) that System (1) exhibits *uniform weak persistence* of the disease when $R_0 > 1$; that is, when $R_0 > 1$, there exists an $\epsilon > 0$ such that $\limsup_{t\to\infty} \sum_{i=1}^{Q} I_i(t) + z_i(t) \geq \epsilon$, for any initial condition for which $\sum_{i=1}^{Q} I_i(0) + z_i(0) > 0$. Furthermore, because our model is an autonomous ordinary differential equation, *uniform weak persistence* implies *uniform strong persistence*. Consequently, when $R_0 > 1$, there exists an $\epsilon > 0$ such that $\liminf_{t\to\infty} \sum_{i=1}^{Q} I_i(t) + z_i(t) \geq \epsilon$, for any initial condition for which $\sum_{i=1}^{Q} I_i(0) > 0$[42, 43]. A generalization of our multi-patch system (see System (8) in [47]) exhibits a unique endemic equilibrium when $R_0 > 1$ which is globally asymptotically stable. Likewise, the disease-free equilibrium for their model is globally asymptotically stable when $R_0 \leq 1$. In fact, Auger *et al.* [47] proved this result even when migration is neither constant across the landscape, nor symmetric.

Because $R_{0,i}$ defines a threshold for disease persistence in an isolated patch and R_0 defines a threshold for disease persistence in the connected network, we use these two quantities as surrogates for local patch persistence when patches are isolated, and persistence in the connected network as a whole, respectively. Prevalence, on the other hand, was calculated as the total proportion of infected hosts in the landscape at equilibrium.

Heterogeneity in transmission intensity was quantified using the coefficient of variation (CV) of the ratio of mosquito to humans (m) such that

$$\mathrm{CV} = \frac{s_{\bar{m}}}{\bar{m}}, \tag{2}$$

where $\bar{m}$ describes the average ratio of mosquito to humans in the landscape and $s_{\bar{m}}$ represents the standard deviation associated with this average. This coefficient of variation is a simple measure commonly used in landscape ecology to quantify landscape heterogeneity [48].

We analyze two cases: (1) a simple two-patch system ($Q = 2$) where we study analytically the relationship between spatial heterogeneity, R_0 and prevalence. Then, (2) we address a similar question in a multi-patch system ($Q = 10$) where each patch is characterized by their unique transmission intensity (see below).

Two-patch analysis

We use an analytical approach (see S3 Text) to study the relationship between R_0, prevalence, and spatial heterogeneity in the special case where the network is composed of two connected patches ($Q = 2$). Transmission heterogeneity in the system is created by choosing different values for m_1 and m_2, the ratio of mosquitoes to humans in the two patches, and quantified by the coefficient of variation, CV. We define $\bar{m}$ to be the average of m_1 and m_2, and study the behavior of R_0 and prevalence as CV increases.

Multi-patch simulation

To study the implications of spatial heterogeneity in transmission intensity, in the presence of host movement, for disease prevalence and persistence, we generated a landscape composed of $Q = 10$ discrete patches connected by movement (Fig 1). We used this landscape to simulate a spatially homogeneous configuration in transmission intensity and four heterogeneous configurations (Fig 1). As with the two-patch analysis, the variation in transmission intensity was attained by varying the ratio of mosquitoes to humans m_i, while keeping all other parameters constant (Table 1). The ratio of mosquitoes to humans in each patch was drawn from a normal distribution such that in the homogeneous configuration $m_i = 60$, and in the four heterogeneous configurations $m_i \overset{iid}{\sim} N(60, 10)$, $m_i \overset{iid}{\sim} N(60, 20)$, $m_i \overset{iid}{\sim} N(60, 30)$, and $m_i \overset{iid}{\sim} N(60, 40)$. This resulted in the same mean transmission intensity in each of the landscape configurations ($\bar{R}_{0,i}$), although the range (min $R_{0,i}$, max $R_{0,i}$ varied among the five configurations: [2.17, 2.17], [1.04, 3.33], [0.03, 4.66], [0.03, 5.96], and [0.03, 6.83] from the homogeneous landscape to the most heterogeneous configuration, respectively (Fig 1). This resembles, in part, variation in malaria transmissibility reported in South America and Africa [1]. To determine how host movement affected persistence and prevalence, and how their relationship depended upon variation in patch transmissibility, we varied the rate of host movement between all patches (k) from 0 to 0.2 (days^{-1}) in 1×10^{-2} increments. This rate was equal among all patches. Given that population size was also equal among patches we are evaluating the simple case where population size is constant and movement is symmetric among patches. We replicated this simulation 100 times for each configuration.

Results

Two-patch analysis

To evaluate the effect of heterogeneity in transmission intensity on disease dynamics, we first proved analytically for the two-patch model that the network reproduction number R_0, and the

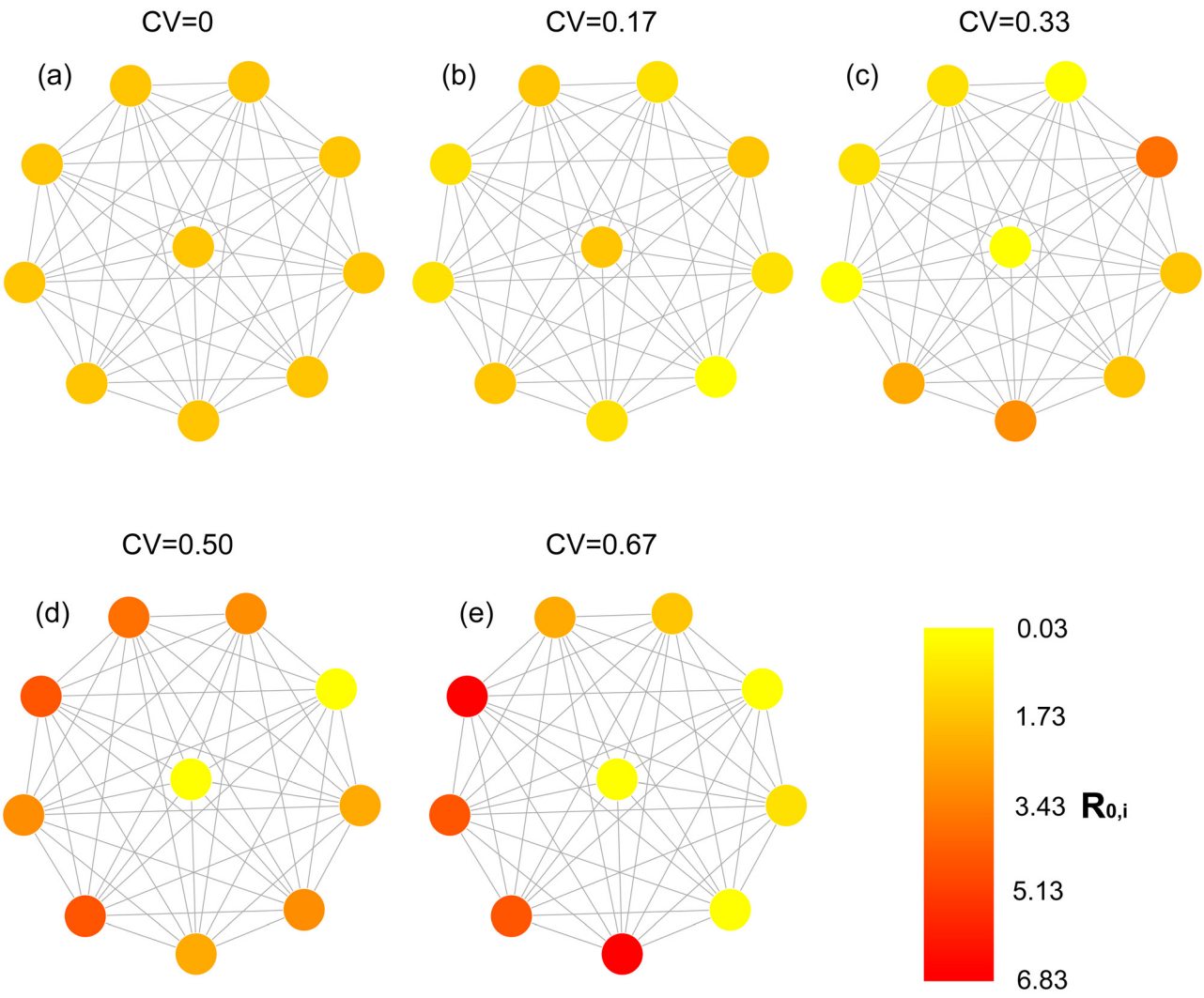

Fig 1. Network representation of simulated landscape configurations. Nodes represent patches characterized by their randomly generated $R_{0,i}$, and links represent host movement. Each configuration represents a particular scenario of spatial heterogeneity in transmission intensity, which increases with increasing coefficient of variation (CV).

doi:10.1371/journal.pone.0127552.g001

Table 1. Parameter values for patches in the simulated landscape. The ratio of mosquitoes to humans varied depending on landscape configuration where $s = 0$ for the homogeneous configuration and $s = \{0.17m, 0.33m, 0.5m, 0.67m\}$ for the spatially heterogeneous configurations.

Parameter	Description	Value	Units	Reference(s)
m	Ratio of mosquitoes to humans	$\sim N(60, s)$	mosquitoes/human	
a	Mosquito biting rate	0.1	bites per mosquito per day	[49]
b	Effective transmission from mosquito to human	0.1	probability	[50]
c	Effective transmission from human to mosquito	0.214	probability	[51, 52]
g	Mosquito per-capita death rate	0.167	probability of mosquito dying per day	[53, 54]
n	Incubation period	10	days	[55, 56]
r	Recovery rate	0.0067	$days^{-1}$	[57]
N	Total population size	9×10^6	number of human hosts	
k	Rate of movement	[0, 0.2]	$days^{-1}$	

doi:10.1371/journal.pone.0127552.t001

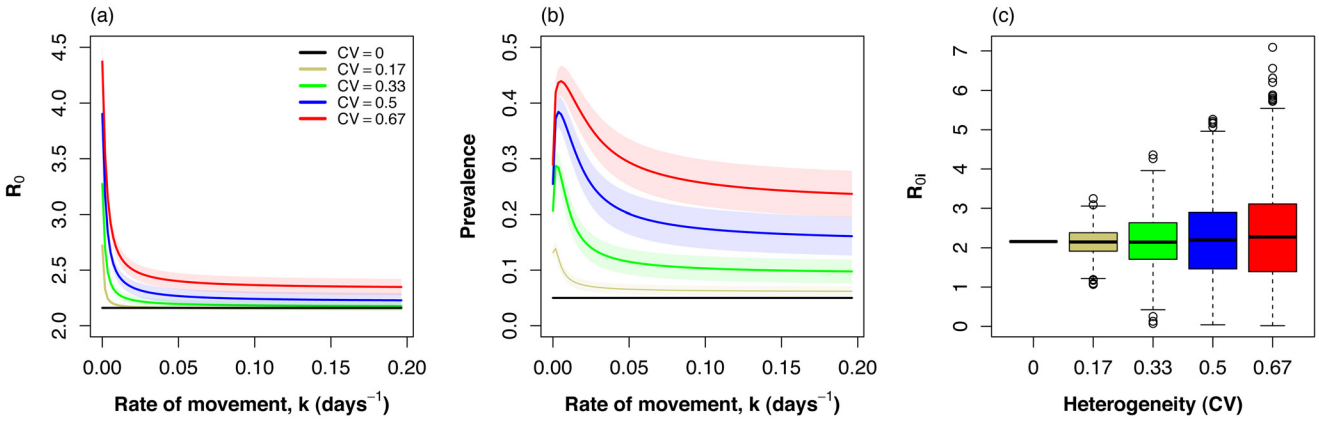

Fig 2. (a) The basic reproduction number R_0 and (b) disease prevalence as a function of increasing movement rate (k) in a spatial network composed of 10 regions with varying levels of heterogeneity in transmission intensity. Lines represent means and shaded areas 95% confidence intervals. Spatial heterogeneity in transmission intensity increases with the coefficient of variation (CV). (c) Box-plots shows the distribution of patch-specific transmission intensities $R_{0,i}$ in 100 simulations for each level of spatial heterogeneity. Note how variance increases with CV, while the average remains similar among configurations.

doi:10.1371/journal.pone.0127552.g002

total disease prevalence $\lim_{t\to\infty}(I_1(t)/N+I_2(t)/N)$ increase with variance $V=\frac{1}{2}\left((m_1-\bar{m})^2+(m_2-\bar{m})^2\right)$, even if $\bar{m}=mean\{m_1,m_2\}$, and consequently the average transmission intensity $(R_{01}+R_{02})/2$ between the two regions, remains constant (see Theorems 0.0.2 and 0.0.4 in S3 Text). Because CV is proportional to the square root of the variance V, this implies that disease persistence and prevalence increase with CV. However, the influence of heterogeneity on R_0 becomes less profound as connectivity between the two patches increases (see Proposition 0.0.3 in S3 Text).

Multi-patch analysis

Spatial heterogeneity in transmission intensity increased long-term persistence of infection (R_0) in the multi-patch system (Fig 2). Yet, increasing host movement-rate decreased R_0 in the spatially heterogeneous scenarios. Spatial homogeneity resulted in the lowest R_0 of all landscape configurations (Fig 2), which is consistent with our conclusions derived analytically from the two-patch system (see above). R_0 in this homogeneous case was also independent of movement because the system was effectively a one patch system. In contrast, in all heterogeneous configurations, increasing host movement-rate resulted in a decrease in R_0 that approached an asymptote. The value of this asymptote increased with increasing spatial heterogeneity (Fig 2), which is also consistent with our analytic results for the two-patch case.

Similarly, spatial heterogeneity in transmission intensity increased disease prevalence in the multi-patch system. Spatial homogeneity in transmission intensity resulted in the lowest prevalence of all landscape configurations (Fig 2). Maximum prevalence and the asymptotic prevalence with increasing spatial heterogeneity in transmission intensity, which again, agrees with our conclusions derived for the two-patch case. Disease prevalence initially increased with increasing movement, was maximized at relatively low movement rates and later decreased. The movement rate, k, that maximized prevalence increased with increasing heterogeneity and occurred at movement rates corresponding to once every 0.5 to 1.5 years. This suggests that the rate of movement required to maximize disease prevalence increases with increasing spatial heterogeneity in transmission intensity. Note that, in the simulations, mean $R_{0,i}$ remained the

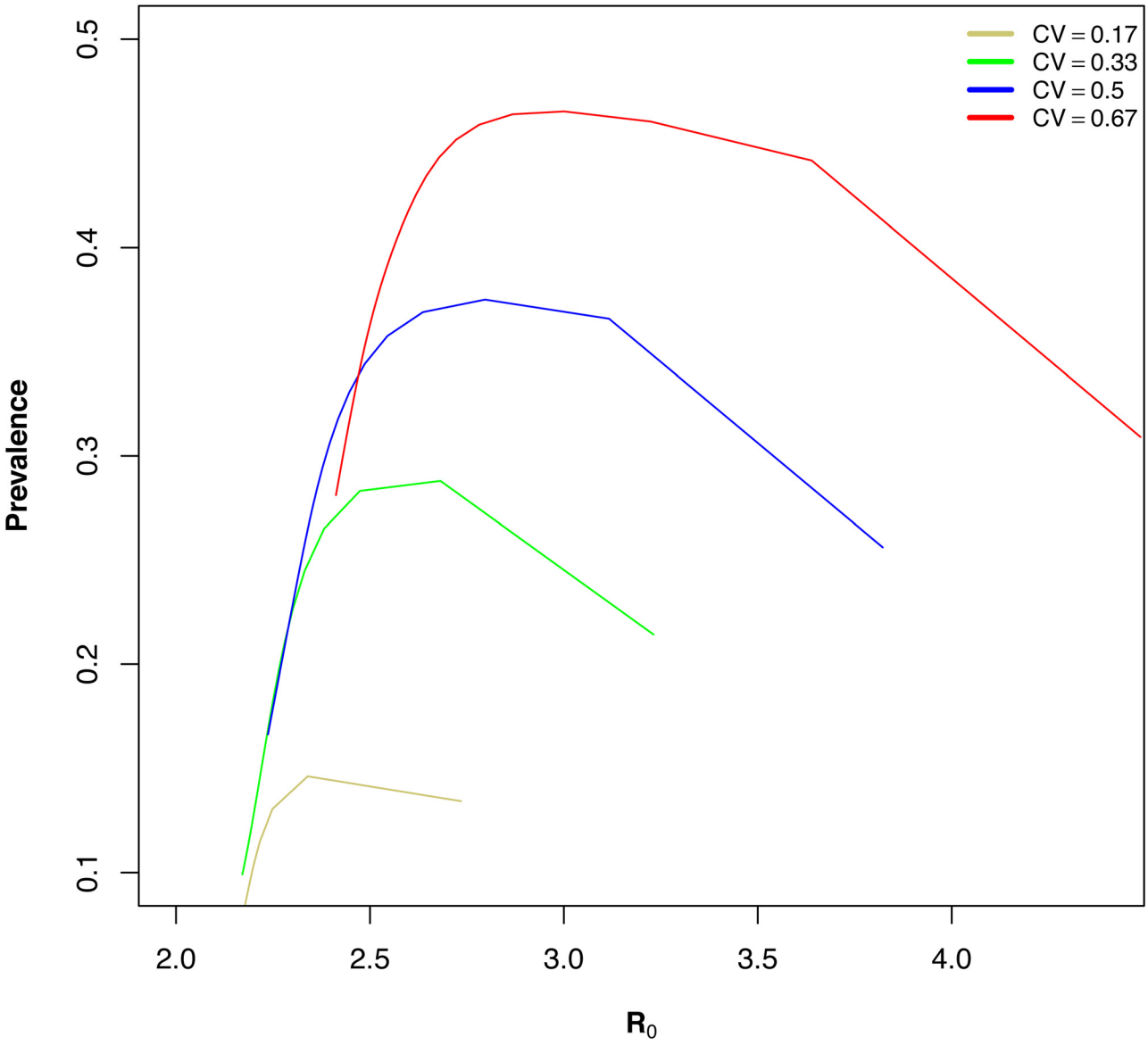

Fig 3. Non-monotonic relationship between R_0 and prevalence. The figure shows four landscape configurations with spatial heterogeneity in transmission intensity for increasing rates of host movement.

doi:10.1371/journal.pone.0127552.g003

same for all scenarios while variance increased with increasing coefficient of variation, as expected (Fig 2). In all heterogeneous configurations prevalence and R_0 followed a non-monotonic relationship in the presence of host movement (Fig 3).

Discussion

We have explored the way that disease prevalence and R_0 — two important measures of mosquito-borne pathogen transmission — display a complex non-monotonic relationship as a result of spatial heterogeneity in mosquito density and human mobility. Heterogeneity in mosquito density and mosquito bionomic patterns affecting vectorial capacity drive spatially

heterogeneous biting patterns, while human mobility connects isolated areas that can have very different mosquito populations. We illustrated these patterns analytically in a two-patch system, and numerically in a multi-patch extension of the Ross-Macdonald modeling framework. We showed that prevalence was maximized at low rates of movement, whereas R_0 always decreased with increasing movement rates. These results suggest that the relationship between R_0 and prevalence is intimately intertwined with the interaction between host movement and the degree of spatial heterogeneity in a region.

Transmission heterogeneity generally promotes persistence in host-parasite systems [18, 58–61]. This heterogeneity may have a spatial component arising from spatial variation in factors affecting mosquito ecology such as habitat distribution or host finding ability [25, 61]. Our results showed that disease persistence decreased with increasing rates of movement even in highly spatially heterogeneous landscapes with multiple transmission hotspots (Figs 1 and 2). At low rates of movement, transmission was highly heterogeneous, with high rates of transmission in some patches and low in others. R_0 was higher in this scenario, because our calculation of R_0 describes the average number of potential infections that arise from an average infected host in the system and thus its magnitude is being influenced by conditions in high transmission patches (Fig 4). Transmission becomes more homogeneous with increasing rate of movement resulting in individual patch transmissibility more similar to the overall average (Fig 4). A similar result was found in a study of the metapopulation dynamics of Schistosomiasis (bilharzia) [62], where increased social connectivity sometimes reduced large-scale disease persistence because as mobility increases infectious individuals spent less time in areas of high transmission distributing infection away from hotspots. Thus, acknowledging host movement patterns is required to better understand disease persistence in heterogeneous landscapes.

Results from our numerical simulations support previous theoretical and empirical work showing that disease prevalence is generally maximized at low to intermediate levels of movement [31, 63, 64]. Our results add to this body of theory by showing that the amount of movement required to achieve peak prevalence increases with increasing spatial transmission heterogeneity. At very low rates of movement, individuals spend most of their time in a single patch. In transmission hotspots most hosts are already infected at equilibrium and most bites do not yield new infections. A relatively small increase in movement will significantly increase the number of hosts exposed to very intense transmission (Fig 4). Therefore, as connectivity increases, the number of infectious bites in high transmission patches decrease, yet, this decrease is offset by the increase in the number of susceptibles that visit these patches. As connectivity continues to increase, hosts spend less time in high transmission patches resulting in a decrease in the number of hosts that become infected in high transmission patches. This causes the number of infectious bites in high transmission patches to decline, ultimately causing fewer people to be infected, and prevalence decreases. The different behaviors of prevalence and R_0 in the presence of spatial heterogeneity and mobility suggest a role for models including mobility and spatial scale in the estimation of prevalence based on R_0 estimates, because the assumed positive relationship between the two is disrupted [21].

Reproduction numbers (R_0) are useful to understand the intensity of transmission in a region and are often used to design and evaluate control measures of mosquito-borne diseases. The estimation of R_0 can be done using several different methods, including estimating number of infectious bites on a person per year [1, 61, 65, 66]. Generally, depending on the assumptions about superinfections and density dependence among parasites, R_0 is proportional to the inverse of the fraction of uninfected individuals at equilibrium (i.e. R_0 and prevalence are positively correlated) [67, 68]. Yet, this relationship between prevalence and R_0 has been shown to be disrupted by heterogeneous biting [18, 58, 61, 67–69]. Our analysis of the two-patch system illustrated that increasing heterogeneity increases both prevalence and R_0, but the multi-patch

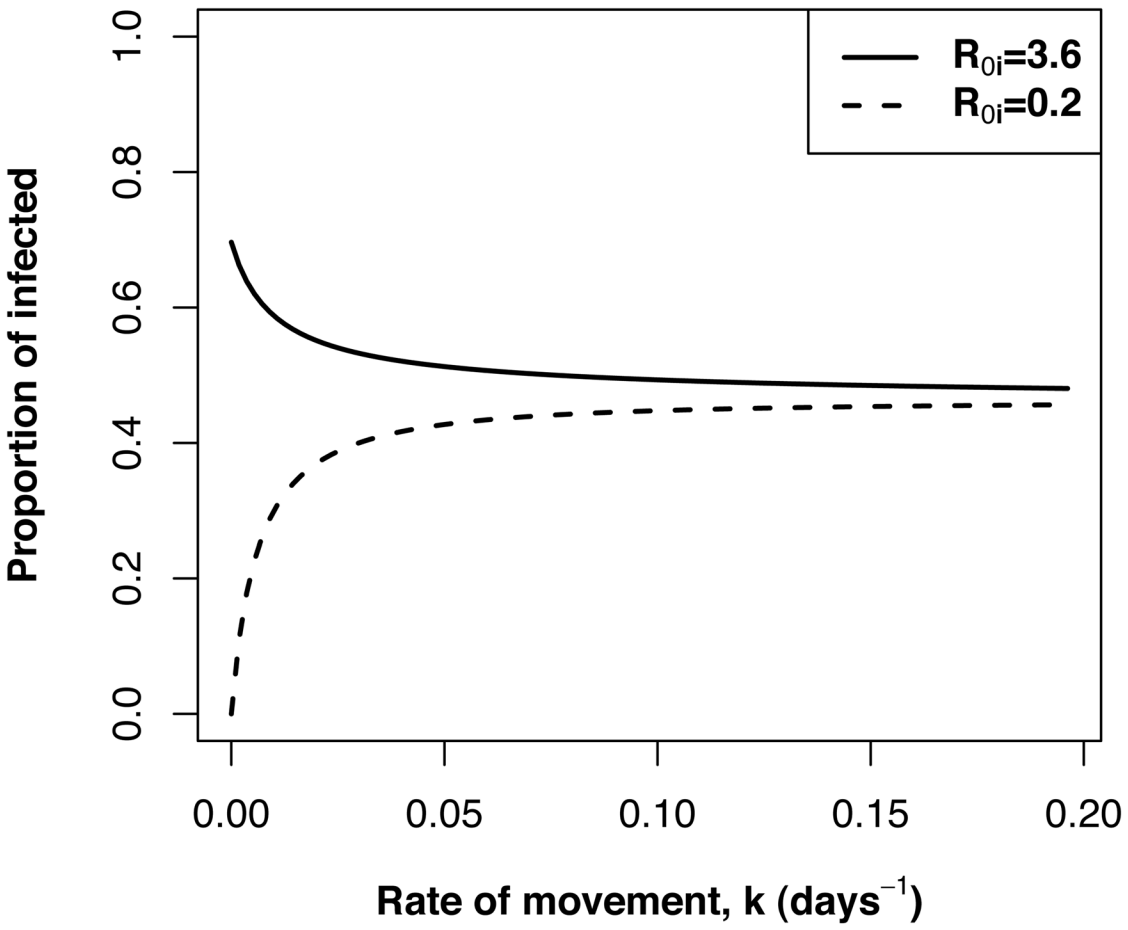

Fig 4. The change in the patch-specific proportion of infected hosts in a high transmission patch ($R_{0,i}$ = 3.6) and a low transmission patch ($R_{0,i}$ = 0.2) as a function of increasing rate of movement. The proportion of infected hosts in the low transmission patch increase with increasing rate of movement because it is receiving infected immigrants from other patches with high transmission. The proportion of infected hosts in the high transmission patch decrease with increasing rate of movement because of increasing emigration of infected hosts to other patches.

doi:10.1371/journal.pone.0127552.g004

numerical simulations show this effect is diminished as connectivity increases suggesting that the human"activity space" — or how humans spend time between areas of varying mosquito densities — is also an important determinant of the relationship between R_0 and prevalence [70]. For example, assuming that transmission intensity across two regions is the average of the transmission intensity in each region will underestimate the disease burden, particularly at low to intermediate levels of connectivity. Therefore our results emphasize the necessity for reasonable estimates of host movement rates, because individual patch transmission intensities do not uniquely determine overall transmission intensity and prevalence.

Our findings have important practical implications for mosquito-borne disease control in heterogeneous landscapes in the presence of symmetric host movement. Our results show that the dynamics of spatially heterogeneous system are driven primarily by the characteristics of areas with the highest potential for transmission by mosquitoes, which supports the idea that hotspots should be targeted for control efforts. If control strategies are untargeted these high transmission areas may represent residual areas where the disease persists with the potential to re-colonize others [32, 71, 72], or maintain transmission throughout the system. This is shown

by the persistence of malaria in many landscape scenarios, despite $R_{0,i} < 1$ in many patches (Fig 2a and 2c). Thus, controlling malaria transmission in areas with heterogeneous transmission requires a combination of interventions that include mosquito control, the reduction of human infectious reservoirs, and vaccination targeted towards high transmission areas [32].

Finally, human movement between areas often changes over time, and predicting how these changes will affect transmission and prevalence requires understanding the effect of connectivity on prevalence and the initial degree of movement. If human movement is very low initially, an increase in movement is likely to increase endemic prevalence, while an initially high human movement will likely result in a decrease in endemicity if movement increases further. Therefore, knowing the degree of connectivity between areas and how connectivity changes over time is also important to management and elimination planning [32]. Recent studies are beginning to analyze human movement in relation to mosquito-borne pathogen transmission [70, 73–75], and these show great promise for improving models of mosquito-borne pathogen transmission across geographic scales.

Supporting Information

S1 Text. Multi-patch model derivation. Derivation of a multi-patch extension of the Ross-Macdonald model in Eq (1) from a single-patch model.
(PDF)

S2 Text. Theorem 0.0.1. Mathematical proof showing that system of equations in (1) exhibit *uniform weak persistence*.
(PDF)

S3 Text. Theorem 0.0.2, Proposition 0.03 and Theorem 0.0.4. Mathematical proofs showing that total equilibrium prevalence in a two-patch system is an increasing function of the variance in transmission intensity.
(PDF)

Acknowledgments

This study greatly benefited from insightful discussions with A. Tatem and C. Cosner. We also thank three anonymous reviewers for their insightful and helpful comments on pervious version of this manuscript. Funding was provided by the National Science Foundation (NSF) Quantitative Spatial Ecology, Evolution, and Environment (QSE^3) Integrative Graduate Education and Research Traineeship Program Grant 0801544 at the University of Florida. MAA was also supported by an NSF Doctoral Dissertation Improvement Grant (DEB-1110441).

Author Contributions

Conceived and designed the experiments: MAA OP KL NR TC MM CO DLS. Performed the experiments: MAA OP KL NR. Analyzed the data: MAA OP KL NR. Contributed reagents/materials/analysis tools: MAA OP KL NR TC MM CO DLS. Wrote the paper: MAA OP KL NR TC MM CO DLS.

References

1. Gething PW, Patil AP, Smith DL, Guerra CA, Elyazar IR, Johnston GL, et al. A new world malaria map: *Plasmodium falciparum* endemicity in 2010. Malaria Journal. 2011; 10:378. doi: 10.1186/1475-2875-10-378 PMID: 22185615

2. Gething PW, Elyazar IRF, Moyes CL, Smith DL, Battle KE, Guerra CA, et al. A long neglected world malaria map: *Plasmodium vivax* endemicity in 2010. PLoS Neglected Tropical Diseases. 2012; 6(9): e1814. doi: 10.1371/journal.pntd.0001814 PMID: 22970336
3. Bhatt S, Gething PW, Brady OJ, Messina JP, Farlow AW, Moyes CL, et al. The global distribution and burden of dengue. Nature. 2013; 496:504–507. doi: 10.1038/nature12060 PMID: 23563266
4. Varmus H, Klausner R, Zerhouni E, Acharva T, Daar AS, Singer PA. Public Health. Grand challenges in global health. Science. 2003; 302:398–399. doi: 10.1126/science.1091769 PMID: 14563993
5. Hay SI, Guerra CA, Tatem AJ, Noor AM, Snow RW. The global distribution and population at risk of malaria: past, present, and future. The Lancet Infectious Diseases. 2004; 4(6):327–336. doi: 10.1016/S1473-3099(04)01043-6 PMID: 15172341
6. Cohen JM, Smith DL, Cotter C, Ward A, Yamey G, Sabot OJ, et al. Malaria resurgence: a systematic review and assessment of its causes. Malaria Journal. 2012; 11(1):122. doi: 10.1186/1475-2875-11-122 PMID: 22531245
7. Chiyaka C, Tatem A, Cohen J, Gething P, Johnston G, Gosling R, et al. The stability of malaria elimination. Science. 2013; 339(6122):909–910. doi: 10.1126/science.1229509 PMID: 23430640
8. Smith DL, Cohen JM, Chiyaka C, Johnston G, Gething PW, Gosling R, et al. A sticky situation: the unexpected stability of malaria elimination. Philosophical Transactions of the Royal Society B: Biological Sciences. 2013; 368(1623):20120145. doi: 10.1098/rstb.2012.0145
9. Tatem AJ, Gething PW, Smith DL, Hay SI. Urbanization and the global malaria recession. Malaria Journal. 2013; 12(1):133. doi: 10.1186/1475-2875-12-133 PMID: 23594701
10. Maudea RJ, Lubella Y, Socheatd D, Yeunge S, Saralambaa S, Pongtavornpinyoa W, et al. The role of mathematical modelling in guiding the science and economics of malaria elimination. International Health. 2010; 2(4):239–246. doi: 10.1016/j.inhe.2010.09.005
11. McKenzie FE, Samba EM. The role of mathematical modeling in evidence-based malaria control. American Journal of Tropical Medicine and Hygiene. 2004; 71(Suppl 2):94–96. PMID: 15331824
12. McKenzie FE. Why model malaria? Parasitology Today. 2000; 16(12):511–516. doi: 10.1016/S0169-4758(00)01789-0
13. Smith DL, Battle KE, Hay SI, Barker CM, Scott TW, McKenzie FE. Ross, Macdonald, and a theory for the dynamics and control of mosquito-transmitted pathogens. PLoS Pathogens. 2012; 8(4):e1002588. doi: 10.1371/journal.ppat.1002588 PMID: 22496640
14. Reiner RC, Perkins TA, Barker CM, Niu T, Chaves LF, Ellis AM, et al. A systematic review of mathematical models of mosquito-borne pathogen transmission: 1970–2010. Journal of The Royal Society Interface. 2013; 10(81):20120921. doi: 10.1098/rsif.2012.0921
15. Anderson RM, May RM. Infectious Diseases of Humans. Dynamics and Control. Oxford University Press; 1992.
16. Zanzibar Malaria Control Program. Malaria elimination in Zanzibar: a feasibility assessment; 2009. [Online; accessed October-2009]. http://www.malariaeliminationgroup.org/sites/default/files/MalariaEliminationZanzibar.pdf.
17. Alonso PL, Brown G, Arevalo-Herrera M, Binka F, Chitnis C, Collins F, et al. A research agenda to underpin malaria eradication. PLoS Medicine. 2011; 8(1):e1000406. doi: 10.1371/journal.pmed.1000406 PMID: 21311579
18. Hasibeder G, Dye C. Population dynamics of mosquito-borne disease: persistence in a completely heterogeneous environment. Theoretical Population Biology. 1988; 33(1):31–53. doi: 10.1016/0040-5809(88)90003-2 PMID: 2897726
19. Rodríguez DJ, Torres-Sorando L. Models of infectious diseases in spatially heterogeneous environments. Bulletin of Mathematical Biology. 2001; 63:547–571. doi: 10.1006/bulm.2001.0231 PMID: 11374305
20. Cosner C, Beier JC, Cantrella RS, Impoinvilc D, Kapitanskia L, Pottsd MD, et al. The effects of human movement on the persistence of vector-borne diseases. Journal of Theoretical Biology. 2009; 258 (4):550–560. doi: 10.1016/j.jtbi.2009.02.016 PMID: 19265711
21. Perkins TA, Scott TW, Le Menach A, Smith DL. Heterogeneity, mixing, and the spatial scales of mosquito-borne pathogen transmission. PLoS Computational Biology. 2013; 9(12):e1003327. doi: 10.1371/journal.pcbi.1003327 PMID: 24348223
22. Qiu Z, Kong Q, Li X, Martcheva M. The vector-host epidemic model with multiple strains in a patchy environment. Journal of Mathematical Analysis and Applications. 2013; 405(1):12–36. doi: 10.1016/j.jmaa.2013.03.042
23. Grenfell BT, Dobson AP. Ecology of infectious disease in natural populations. Cambridge University Press; 1995.

24. Torres-Sorando L, Rodríguez DJ. Models of spatio-temporal dynamics in malaria. Ecological Modelling. 1997; 104:231–240. doi: 10.1016/S0304-3800(97)00135-X

25. Smith DL, Dushoff J, McKenzie FE. The risk of mosquito-borne infection in a heterogeneous environment. PLoS Biology. 2004; 2(11):e368. doi: 10.1371/journal.pbio.0020368 PMID: 15510228

26. Woolhouse ME, Dye C, Etard JF, Smith T, Charlwood JD, Garnett GP, et al. Heterogeneities in the transmission of infectious agents: implications for the design of control programs. Proceedings of the National Academy of Sciences USA. 1997; 94(1):338–342. doi: 10.1073/pnas.94.1.338

27. Shaw DJ, Grenfell BT, Dobson AP. Patterns of macroparasite aggregation in wildlife host populations. Parasitology. 1998; 117:597–610. doi: 10.1017/S0031182098003448 PMID: 9881385

28. Smith DL, Drakeley CJ, Chiyaka C, Hay SI. A quantitative analysis of transmission efficiency versus intensity for malaria. Nature Communications. 2010; 1:108. doi: 10.1038/ncomms1107 PMID: 21045826

29. Mbogo CM, Mwangangi JM, Nzovu J, Gu W, Yan G, Gunter JT, et al. Spatial and temporal heterogeneity of *Anopheles* mosquitoes and *Plasmodium falciparum* transmission along the Kenyan coast. American Journal of Tropical Medicine and Hygien. 2003; 68(6):734–742.

30. Kazembe LN, Kleinschmidt I, Holtz TH, Sharp BL. Spatial analysis and mapping of malaria risk in Malawi using point-referenced prevalence of infection data. International Journal of Health Geographics. 2006; 5:41. doi: 10.1186/1476-072X-5-41 PMID: 16987415

31. Adams B, Kapan DD. Man bites mosquito: Understanding the contribution of human movement to vector-borne disease dynamics. PLoS ONE. 2009; 4(8):e6763. doi: 10.1371/journal.pone.0006763 PMID: 19707544

32. Bousema T, Griffin JT, Sauerwein RW, Smith DL, Churcher TS, Takken W, et al. Hitting hotspots: spatial targeting of malaria for control and elimination. PLoS Medicine. 2012; 9(1):e1001165. doi: 10.1371/journal.pmed.1001165 PMID: 22303287

33. Hotez PJ, Molyneux DH, Fenwick A, Kumaresan J, Ehrlich S, Sachs JD, et al. Control of neglected tropical diseases. The New England Journal of Medicine. 2007; 357(10):1018–1027. doi: 10.1056/NEJMra064142 PMID: 17804846

34. Lambrechts L, Knox TB, Wong J, Liebman KA, Albright RG, Stoddard ST. Shifting priorities in vector biology to improve control of vector-borne disease. Tropical Medicine and International Health. 2009; 14 (12):1505–1514. doi: 10.1111/j.1365-3156.2009.02401.x PMID: 19807899

35. Miranda-Franco R, Casta-Vélez A. La erradicación de la malaria en Puerto Rico. Revista Panamericana de Salud Pública. 1997; 2(2):146–150. doi: 10.1590/S1020-49891997000800015 PMID: 9312420

36. Stratton L, O'Neill MS, Kruk ME, Bell ML. The persistent problem of malaria: Addressing the fundamental causes of a global killer. Social Science and Medicine. 2008; 67(5):854–862. doi: 10.1016/j.socscimed.2008.05.013 PMID: 18583009

37. Barbu C, Dumonteil E, Gourbière S. Evaluation of spatially targeted strategies to control non-domiciliated *Triatoma dimidiata* vector of Chagas disease. PLoS Neglected Tropical Diseases. 2011; 5(5): e1045. doi: 10.1371/journal.pntd.0001045 PMID: 21610862

38. Baragatti M, Fournet F, Henry MC, Assi S, Ouedraogo H, Rogier C, et al. Social and environmental malaria risk factors in urban areas of Ouagadougou, Burkina Faso. Malaria Journal. 2009; 8:30. doi: 10.1186/1475-2875-8-13

39. Hernández-Avila JE, Rodríguez MH, Betanzos-Reyes AF, Danis-Lozano R, Méndez-Galván J, Vel azquez-Monroy OJ, et al. Determinant factors for malaria transmission on the coast of Oaxaca State, the main residual transmission focus in México. Salud Pública de México. 2006; 48(5):405–417. PMID: 17063824

40. Grenfell B, Harwood J. (Meta)population dynamics of infectious diseases. Trends in Ecology and Evolution. 1997; 12(10):395–399. doi: 10.1016/S0169-5347(97)01174-9 PMID: 21238122

41. Smith DL, McKenzie FE, Snow RW, Hay SI. Ross, Macdonald, and a theory for the dynamics and control of mosquito-transmitted pathogens. PLoS Pathogens. 2012; 8:e1002588. doi: 10.1371/journal.ppat.1002588 PMID: 22496640

42. Freedman H, Moson P. Persistence definitions and their connections. Proceedings of the american mathematical society. 1990; 109(4):1025–1033. doi: 10.1090/S0002-9939-1990-1012928-6

43. Thieme HR. Persistence under relaxed point-dissipativity (with application to an endemic model). SIAM Journal on Mathematical Analysis. 1993; 24(2):407–435. doi: 10.1137/0524026

44. Prosper O, Ruktanonchai N, Martcheva M. Assessing the role of spatial heterogeneity and human movement in malaria dynamics and control. Journal of Theoretical Biology. 2012; 303:1–14. doi: 10.1016/j.jtbi.2012.02.010 PMID: 22525434

45. Diekmann O, Heesterbeek JAP, Metz JAJ. On the definition and the computation of the basic reproduction ratio R0 in models for infectious diseases in heterogeneous populations. Journal of Mathematical Biology. 1990; 28:365–382. doi: 10.1007/BF00178324 PMID: 2117040

46. van den Driessche P, Watmough J. Reproduction numbers and sub-threshold endemic equilibria for compartmental models of disease transmission. Mathematical Biosciences. 2002; 180(1–2):29–48. doi: 10.1016/S0025-5564(02)00108-6 PMID: 12387915

47. Auger P, Kouokam E, Sallet G, Tchuente M, Tsanou B. The Ross-Macdonald model in a patchy environment. Mathematical Biosciences. 2008; 216(2):123–131. doi: 10.1016/j.mbs.2008.08.010 PMID: 18805432

48. Li H, Reynolds J. On definition and quantification of heterogeneity. Oikos. 1995; 73:280–284. doi: 10.2307/3545921

49. Loyola EG, González-Cerón L, Rodríguez MH, Arredondo-Jiménez JI, Bennett S, Bown DN. *Anopheles albimanus* (Diptera: Culicidae) Host Selection Patterns in Three Ecological Areas of the Coastal Plains of Chiapas, Southern Mexico. Journal of Medical Entomology. 1993; 30:518–523. doi: 10.1093/jmedent/30.3.518 PMID: 8510111

50. Beier JC, Davis JR, Vaughan JA, Noden BH, Beier MS. Quantitation of *Plasmodium falciparum* sporozoites transmitted in vitro by experimentally infected *Anopheles gambiae* and *Anopheles stephensi*. American Journal of Tropical Medicine and Hygiene. 1991; 44:564–570. PMID: 2063960

51. Bonnet S, Gouagna C, Safeukui I, Meunier JY, Boudin C. Comparison of artificial membrane feeding with direct skin feeding to estimate infectiousness of *Plasmodium falciparum* gametocyte carriers to mosquitoes. Transactions of the Royal Society of Tropical Medicine and Hygiene. 2000; 94:103–106. doi: 10.1016/S0035-9203(00)90456-5 PMID: 10748913

52. Collins WE, Warren M, Skinner JC, Richardson BB, Kearse TS. Infectivity of the Santa Lucia (El Salvador) strain of *Plasmodium falciparum* to different anophelines. Journal of Parasitology. 1977; 63:57–61. doi: 10.2307/3280103 PMID: 403273

53. Graves PM, Burkot TR, Saul AJ, Hayes RJ, Carter R. Estimation of anopheline survival rate, vectorial capacity and mosquito infection probability from malaria vector infection rates in villages near Madang, Papua New Guinea. Journal of Applied Ecology. 1990; 27:134–147. doi: 10.2307/2403573

54. Rodríguez MH, Bown DN, Arredondo-Jiménez JI, Villarreal C, Loyola EG, Frederickson CE. Gonotrophic cycle and survivorship of *Anopheles albimanus* (Diptera: Culicidae) in southern Mexico. Journal of Medical Entomology. 1992; 29:395–399. doi: 10.1093/jmedent/29.3.395 PMID: 1625288

55. Bekessy A, Molineaux L, Storey J. Estimation of incidence and recovery rates of *Plasmodium falciparum* parasitaemia from longitudinal data. Bulletin of the World Health Organization. 1976; 54:685–693. PMID: 800968

56. Molineaux L, Gramiccia G. The Garki project: research on the epidemiology and control of malaria in the Sudan savanna of West Africa. WHO Publications, Albany, NY, USA; 1980.

57. Collins WE, Jeffery GM. A retrospective examination of mosquito infection on humans infected with *Plasmodium falciparum*. American Journal of Tropical Medicine and Hygiene. 2003; 68:366–371. PMID: 12685646

58. Dye C, Hasibeder G. Population dynamics of mosquito-borne disease: effects of flies which bite some people more frequently than others. Transactions of the Royal Society of Tropical Medicine and Hygiene. 1986; 80:69–77. doi: 10.1016/0035-9203(86)90199-9 PMID: 3727001

59. Jansen VAA, Lloyd AL. Local stability analysis of spatially homogeneous solutions of multi-patch systems. Journal of Mathematical Biology. 2000; 41:232–252. doi: 10.1007/s002850000048 PMID: 11072757

60. Formont E, Pontier D, Langlais M. Disease propagation in connected host populations with density-dependent dynamics: the case of Feline Leukemia Virus. Journal of Theoretical Biology. 2003; 223:465–475. doi: 10.1016/S0022-5193(03)00122-X

61. Smith DL, Battle KE, Hay SI, Barker CM, Scott TW. Revisiting the basic reproductive number for malaria and its implications for malaria control. PLoS Biology. 2007; 5:e42. doi: 10.1371/journal.pbio.0050042 PMID: 17311470

62. Gurarie D, Seto YW. Connectivity sustains disease transmission in environments with low potential for endemicity: modelling schistosomiasis with hydrologic and social connectivities. Journal of the Royal Society Interface. 2009; 6:495–508. doi: 10.1098/rsif.2008.0265

63. Hess G. Disease in metapopulation models: implications for conservation. Ecology. 1996; 77:1617–1632. doi: 10.2307/2265556

64. McCallum H, Dobson A. Disease and connectivity. In: Connectivity Conservation. Cambridge University Press; 2006. p. 479–501.

65. Smith D, McKenzie FE. Statics and dynamics of malaria infection in *Anopheles* mosquitoes. Malaria Journal. 2004; 3(1):13. doi: 10.1186/1475-2875-3-13 PMID: 15180900

66. Dietz K. The estimation of the basic reproduction number for infectious diseases. Statistical Methods in Medical Research. 1993; 2(1):23–41. doi: 10.1177/096228029300200103 PMID: 8261248

67. Dietz K. Models for vector-borne parasitic diseases. Lecture Notes in Biomathematics. 1980; 39:264–277. doi: 10.1007/978-3-642-93161-1_15

68. Dietz K, Wernsdorfer W, McGregor I. Mathematical models for transmission and control of malaria. Malaria: principles and practice of malariology Volume 2. 1988;p. 1091–1133.

69. Smith DL, Dushoff J, Snow RW, Hay SI. The entomological inoculation rate and its relation to prevalence of *Plasmodium falciparum* infection in African children. Nature. 2005; 438:492–495. doi: 10.1038/nature04024 PMID: 16306991

70. Stoddard ST, Morrison AC, Vazquez-Prokopec GM, Soldan VP, Kochek TJ, Kitron U, et al. The role of human movement in the transmission of vector-borne pathogens. PLoS Neglected Tropical Diseases. 2009; 3(7):e481. doi: 10.1371/journal.pntd.0000481 PMID: 19621090

71. Bautista CT, Chan AS, Ryan JR, Calampa C, Roper MH, Hightower AW, et al. Epidemiology and spatial analysis of malaria in the Northern Peruvian Amazon. American Journal of Tropical Medicine and Hygiene. 2006; 75:1216–1222. PMID: 17172396

72. Ernst KC, Adoka SO, Kowuor DO, Wilson ML, John CC. Malaria hotspot areas in a highland Kenya site are consistent in epidemic and non-epidemic years and are associated with ecological factors. Malaria Journal. 2006; 5:78. doi: 10.1186/1475-2875-5-78 PMID: 16970824

73. Eagle N, Pentland A, Lazer D. Inferring friendship network structure by using mobile phone data. Proceedings of the National Academy of Sciences. 2009; 106:15274–15278. doi: 10.1073/pnas.0900282106

74. Weslowski A, Eagle N, Noor AM, Snow RW, Buckee CO. Heterogeneous mobile phone ownership and usage patterns in Kenya. PLoS ONE. 2012; 7(4):e35319. doi: 10.1371/journal.pone.0035319

75. Wesolowski A, Eagle N, Tatem AJ, Smith DL, Noor AM, Snow RW, et al. Quantifying the impact of human mobility on malaria. Science. 2012; 338(6104):267–270. doi: 10.1126/science.1223467 PMID: 23066082

Spatial heterogeneity, host movement and vector-borne disease transmission

Miguel A. Acevedo[1,*], Olivia Prosper[2], Kenneth Lopiano[3], Nick Ruktanonchai[4], T. Trevor Caughlin[4], Maia Martcheva[5], Craig W. Osenberg[4], David L. Smith[6].

1 University of Puerto Rico–Río Piedras, Department of Biology, San Juan, PR, USA

2 Dartmouth College, Department of Mathematics, Hanover, NH, USA

3 Statistical and Applied Mathematical Sciences Institute, Research Triangle Park, NC, USA

4 University of Florida, Department of Biology, Gainesville, FL, USA

5 University of Florida, Department of Mathematics, Gainesville, FL, USA

6 Department of Epidemiology and Malaria Research Institute, John Hopkins Bloomberg School of Public Health, Baltimore, MD, USA

∗ **E-mail: miguel.acevedo7@upr.edu**

Supporting Information 1

The Ross-Macdonald model describes the proportion of humans infected (i) and the proportion of mosquitoes infected (z) over time:

$$\frac{dz}{dt} = aci(1-z) - gz \tag{1}$$

$$\frac{di}{dt} = mabz(1-i) - ri, \tag{2}$$

where $1-z$ and $1-i$ describe the proportion of susceptible mosquitoes and susceptible humans respectively.

We modified the Ross-Macdonald model [1] to account for the change in the number of humans infected (instead of the proportion), leading to the following set of equations:

$$\frac{dz}{dt} = ac\frac{I}{N}(1-z) - gz \tag{3}$$

$$\frac{dI}{dt} = mabz(N-I) - rI, \tag{4}$$

where N is the total size of the human population of interest, and I is the number of humans infected with malaria. Thus, $N - I$ represents the number of humans who are susceptible.

The parameter a is the rate mosquitoes bite humans, c is the probability a mosquito becomes infected given that the mosquito has bitten an infected human, b is the probability a susceptible human being was infected given a mosquito bite from an infected mosquito, g is the mosquito death rate, m is the ratio of the abundance of mosquitoes to humans and r is the recovery rate of infected humans. In this model there is no immunity after infection. Because the model without human demography is asymptotically equivalent to the model with demography, and because we are interested in equilibrium behavior, we omitted human births and deaths for simplicity.

We have incorporated two modifications to the original model. First, given the high mortality rate of mosquitoes, many may not survive to become infectious; hence we replaced $(1 - z)$ with $e^{-gn} - z$ [2], where n is the extrinsic incubation period.

Second, we incorporated immigration and emigration between all Q patches resulting in the following system of $3 \times Q$ equations:

$$\frac{dz_i}{dt} = a_i c_i \frac{I_i}{N_i}(e^{-g_i n_i} - z_i) - g_i z_i \tag{5}$$

$$\frac{dI_i}{dt} = m_i a_i b_i z_i (N_i - I_i) - r_i I_i - I_i \sum_{j \neq i}^{Q} k_{ji} + \sum_{j \neq i}^{Q} k_{ij} I_j \tag{6}$$

$$\frac{dN_i}{dt} = -N_i \sum_{j \neq i}^{Q} k_{ji} + \sum_{j \neq i}^{Q} k_{ij} N_j \tag{7}$$

Under the assumptions specified in the main manuscript, our model simplifies to:

$$\begin{aligned} \frac{dz_i}{dt} &= ac \frac{I_i}{N}(e^{-gn} - z_i) - g z_i \\ \frac{dI_i}{dt} &= m_i a b z_i (N - I_i) - r I_i - I_i \sum_{j \neq i}^{Q} k + \sum_{j \neq i}^{Q} k I_j \end{aligned} \tag{8}$$

References

1. Bailey NTJ (1982) The biomathematics of malaria. Oxford University Press.

2. Smith D, McKenzie F (2004) Statics and dynamics of malaria infection in *Anopheles* mosquitoes.

35 Malaria Journal 3: 13.

Spatial heterogeneity, host movement and vector-borne disease transmission

Miguel A. Acevedo[1,*], Olivia Prosper[2], Kenneth Lopiano[3], Nick Ruktanonchai[4], T. Trevor Caughlin[4], Maia Martcheva[5], Craig W. Osenberg[4], David L. Smith[6].

1 University of Puerto Rico–Río Piedras, Department of Biology, San Juan, PR, USA

2 Dartmouth College, Department of Mathematics, Hanover, NH, USA

3 Statistical and Applied Mathematical Sciences Institute, Research Triangle Park, NC, USA

4 University of Florida, Department of Biology, Gainesville, FL, USA

5 University of Florida, Department of Mathematics, Gainesville, FL, USA

6 Department of Epidemiology and Malaria Research Institute, John Hopkins Bloomberg School of Public Health, Baltimore, MD, USA

∗ **E-mail: miguel.acevedo7@upr.edu**

Supporting Information 2

Theorem 0.0.1. *If $R_0 > 1$, System (1) in the main text exhibits uniform weak persistence; that is, there exists an $\epsilon > 0$ such that*

$$\limsup_{t\to\infty} \sum_{i=1}^{Q} I_i(t) + z_i(t) \geq \epsilon,$$

whenever $\sum_{i=1}^{Q} I_i(0) + z_i(0) > 0$.

Proof. By way of contradiction, suppose $\limsup_{t\to\infty} \sum_{i=1}^{Q} I_i(t) + z_i(t) < \epsilon$ for all $\epsilon > 0$. Then, $I_i(t) \leq \epsilon$ and $z_i(t) \leq \epsilon$ for all t, and for each $i = 1, 2, \ldots, Q$. From System 1 in the main text, we obtain the following inequalities:

$$\frac{dI_i(t)}{dt} \geq \xi_i(\epsilon) z_i - [r + (Q-1)k] I_i + k \sum_{j\neq i}^{Q} I_j$$

$$\frac{dz_i(t)}{dt} \geq \eta_i(\epsilon) I_i - g z_i, \quad i = 1, \ldots, Q$$

where $\xi_i(\epsilon) = m_i ab(N-\epsilon)$ and $\eta_i(\epsilon) = ac\frac{I_i}{N}(e^{-gn}-\epsilon)$. Note that

$$\frac{dX_i(t)}{dt} = \xi_i(\epsilon)y_i - [r+(Q-1)k]X_i + k\sum_{j\neq i}^{Q} X_j$$
$$\frac{dy_i(t)}{dt} = \eta_i(\epsilon)X_i - gy_i, \quad i = 1,\ldots,Q$$

is a linear system of $2Q$ equations, and can be written in the form $\mathbf{W}' = J(\epsilon)\mathbf{W}$, where

$$\mathbf{W} = (y_1, y_2, \ldots, y_Q, X_1, X_2, \ldots, X_Q)^T,$$

and

$$J(\epsilon) = \begin{bmatrix} J_{1,1} & J_{1,2}(\epsilon) \\ J_{2,1}(\epsilon) & J_{2,2} \end{bmatrix},$$

where each $J_{i,j}$ is a $Q\times Q$ block matrix defined by $J_{1,1} = diag(-g,-g,\ldots,-g)$, $J_{1,2}(\epsilon) = diag(\eta_1(\epsilon),\eta_2(\epsilon),\ldots,\eta_Q(\epsilon))$, $J_{2,1}(\epsilon) = diag(\xi_1(\epsilon),\xi_2(\epsilon),\ldots,\xi_Q(\epsilon))$, and

$$J_{2,2}(\epsilon) = \begin{bmatrix} -[r+(Q-1)k] & k & \cdots & k \\ k & -[r+(Q-1)k] & \cdots & k \\ \vdots & \vdots & \ddots & \vdots \\ k & k & \cdots & -[r+(Q-1)k] \end{bmatrix}.$$

Because $\xi_i(0) = m_i abN = \alpha_i N$ and $\eta_i(0) = \dfrac{ace^{-gn}}{N} = \dfrac{\beta}{N}$, $J(0)$ is precisely the Jacobian of System (1) in the main text evaluated at the disease-free equilibrium. Furthermore, $I_i(t) \geq X_i(t)$ for all t and for each i, provided they have the same initial conditions.

Let $F(\epsilon)$ and V be such that $F(\epsilon) = \begin{bmatrix} 0 & J_{1,2}(\epsilon) \\ J_{2,1}(\epsilon) & 0 \end{bmatrix}$, and $V = \begin{bmatrix} J_{1,1} & 0 \\ 0 & J_{2,2} \end{bmatrix}$. Then, $J(\epsilon) = F(\epsilon) - V$.

Let $R(\epsilon) := (\rho(F(\epsilon)V^{-1}))^2$, the square of the spectral radius of the matrix FV^{-1}. Then, $\lim_{\epsilon\to 0} R(\epsilon) = R_0$. Because $R_0 > 1$, this implies that there exists an $\epsilon' > 0$ such that $R(\epsilon') > 1$. Because $F(\epsilon')$ is nonnegative and V is a non-singular M-matrix, $\rho(F(\epsilon')V^{-1}) > 1$ implies that at least one eigenvalue lies in the

right half of the complex plane. Hence, the spectrum of $J(\epsilon')$ has an eigenvalue with positive real part, implying that $\lim_{t\to\infty} I_i(t) = \infty$ or $\lim_{t\to\infty} z_i(t) = \infty$ for some i, which is a contradiction. Therefore, the conclusion of the theorem holds.

□

Spatial heterogeneity, host movement and vector-borne disease transmission

Miguel A. Acevedo[1,*], Olivia Prosper[2], Kenneth Lopiano[3], Nick Ruktanonchai[4], T. Trevor Caughlin[4], Maia Martcheva[5], Craig W. Osenberg[4], David L. Smith[6].

1 University of Puerto Rico–Río Piedras, Department of Biology, San Juan, PR, USA

2 Dartmouth College, Department of Mathematics, Hanover, NH, USA

3 Statistical and Applied Mathematical Sciences Institute, Research Triangle Park, NC, USA

4 University of Florida, Department of Biology, Gainesville, FL, USA

5 University of Florida, Department of Mathematics, Gainesville, FL, USA

6 Department of Epidemiology and Malaria Research Institute, John Hopkins Bloomberg School of Public Health, Baltimore, MD, USA

∗ **E-mail: miguel.acevedo7@upr.edu**

Supporting Information 3

Two-patch analysis

We first made the following assumptions:

1. Each patch has identical parameters, with the exception of the ratio of mosquitoes to humans m_1 and m_2.

2. $\bar{m} := \frac{m_1+m_2}{2}$, the average of m_1 and m_2, is fixed.

3. $\bar{\alpha} := \frac{m_1}{m_2}$, where, without loss of generality, $m_1 > m_2$ so that $\alpha \in (1, \infty)$.

Theorem 0.0.1. *Under the above assumptions, R_0 is an increasing function of the variance*

$$V = \frac{(m_1 - \bar{m})^2 + (m_2 - \bar{m})^2}{2}.$$

Proof. Note that $\dfrac{\partial R_0}{\partial V} = \dfrac{\partial \bar{\alpha}}{\partial V} \cdot \dfrac{\partial R_0}{\partial \bar{\alpha}}$. We will first show that $\dfrac{\partial R_0}{\partial \bar{\alpha}} > 0$.

Assumptions 2 and 3 imply that

$$(m_1, m_2) = \left(\frac{2\bar{\alpha}\bar{m}}{\bar{\alpha}+1}, \frac{2\bar{m}}{\bar{\alpha}+1} \right). \tag{1}$$

Using the definition of R_0 described in the previous section, it is straightforward to show that R_0 for our two-patch system is a special case of the R_0 derived in [1]. In [1],

$$R_0 = \frac{1}{2\sigma}\left(s_1 t_2 + s_2 t_1 + \sqrt{(s_1 t_2 + s_2 t_1)^2 - 4 s_1 s_2 \sigma} \right),$$

where $\sigma = k_{12}r_1 + k_{21}r_2 + r_1 r_2$, $s_i = \frac{\alpha_i \beta_i}{g_i}$, and $t_i = r_i + k_{ji}$. Since all patch parameters, except for m_1 and m_2 are identical in this manuscript, we take $k = k_{12} = k_{21}$, $r = r_1 = r_2$, $\beta = \beta_1 = \beta_2$, and $g = g_1 = g_2$. Subsequently, we have $\sigma = 2kr + r^2$, $s_i = \frac{\alpha_i \beta}{g}$, and $t = r + k = t_1 = t_2$.

Note that $s_1 t_2 + s_2 t_1 = s_2 t_2 \left(\frac{s_1}{s_2} + \frac{t_1}{t_2} \right) = s_2 t_2 (\bar{\alpha} + 1)$. So, $R_0 = \frac{s_2 t}{2\sigma}\left(\bar{\alpha} + 1 + \sqrt{(\bar{\alpha}+1)^2 - 4\bar{\alpha}\frac{\sigma}{t^2}} \right)$.

Recall that $s_2 = m_2 \eta$, where $\eta = a^2 b c e^{-gn}/g$ (under the simplifying parameter assumptions). From the expression for m_2, we obtain $s_2 = \frac{2\eta\bar{m}}{\bar{\alpha}+1}$, which yields (after simplification) an expression for R_0 as a function of $\bar{\alpha}$:

$$R_0(\bar{\alpha}) = \eta \bar{m} \frac{t}{\sigma}\left(1 + \sqrt{1 - 4\frac{\bar{\alpha}}{(\bar{\alpha}+1)^2} \cdot \frac{\sigma}{t^2}} \right).$$

Now, it remains to show that $\frac{\partial R_0}{\partial \bar{\alpha}} > 0$ on $(1, \infty)$. Only the argument of the square root in R_0 depends on $\bar{\alpha}$. Thus, to determine the sign of $\frac{\partial R_0}{\partial \bar{\alpha}}$, we first note that $\frac{\partial}{\partial \bar{\alpha}}\left(\frac{\bar{\alpha}}{(\bar{\alpha}+1)^2} \right) = \frac{1-\bar{\alpha}}{(\bar{\alpha}+1)^3} < 0$ on $(1, \infty)$. From this, it is clear that R_0 is an increasing function of $\bar{\alpha}$.

We conclude the proof by writing V as a function of $\bar{\alpha}$, and illustrating that $\frac{\partial \bar{\alpha}}{\partial V}$ is also positive. Substituting Equation (1) into the expression for the two-patch variance V, we find that $V(\bar{\alpha}+1)^2 = \bar{m}^2(\bar{\alpha}-1)^2$. Implicit differentiation with respect to V, and treating $\bar{\alpha}$ as a function of V, yields:

$$\frac{\partial \bar{\alpha}}{\partial V} = \frac{(\bar{\alpha}+1)^3}{4\bar{m}^2(\bar{\alpha}-1)},$$

which is positive. In the above calculation, we used the fact that $V(\bar{\alpha}+1)^2 = \bar{m}^2(\bar{\alpha}-1)^2$ to write the expression in terms of only $\bar{m}$ and $\bar{\alpha}$. Consequently, R_0 is an increasing function of V.

□

Proposition 0.0.2. $\frac{\partial}{\partial k}\frac{\partial R_0}{\partial \bar{\alpha}} < 0$.

Proof. Calculating $R_0'(\bar{\alpha})$ explicitly, we obtain: $R_0'(\bar{\alpha}) = 2\eta\bar{m}\left(1 - 4\frac{\bar{\alpha}}{(\bar{\alpha}+1)^2}\cdot\frac{\sigma}{t^2}\right)^{-\frac{1}{2}}\cdot\frac{\bar{\alpha}-1}{(\bar{\alpha}+1)^3}\cdot\frac{1}{t}$. Clearly, $\frac{\partial}{\partial k}\left(\frac{1}{t}\right) < 0$ since $t = r + k$, and $\frac{\partial}{\partial k}\left(\frac{\sigma}{t^2}\right) = -\frac{2rk}{(r+k)^3} < 0$. Since $1/t$ and σ/t^2 are both decreasing functions of k and no other terms in $\frac{\partial R_0}{\partial\bar{\alpha}}$ depend on k, we observe that $\frac{\partial R_0}{\partial\bar{\alpha}}$ must decrease with k.

□

Theorem 0.0.3. *The total equilibrium prevalence in the two-patch system, $I^* = I_1^* + I_2^*$ is an increasing function of the variance V.*

Proof. The equilibrium equations for our two-patch system are

$$0 = ac\frac{I_i}{N}(e^{-gn} - z_i) - gz_i, \quad i = 1, 2$$
$$0 = m_i abz_i(N - I_i) - rI_i - kI_i + kI_j, \quad i = 1, 2$$

Solving for z_i in the first equation and substituting this quantity into the second equation, we obtain the equilibrium equations

$$0 = \frac{m_i a^2 bce^{-gn}}{acI_i + gN}(N - I_i) - (r + k)I_i + kI_j, \quad i = 1, 2,$$

which is a special case of the equilibrium equations in [1].

From equations (33)-(34) in [1],

$$\frac{\partial I_1^*}{\partial\alpha_1} = -\frac{C_{\alpha_1}A_2}{A_1A_2 - B_1B_2} \tag{2}$$
$$\frac{\partial I_2^*}{\partial\alpha_1} = \frac{C_{\alpha_1}B_2}{A_1A_2 - B_1B_2}, \tag{3}$$

where

$$\begin{aligned} A_i &= \alpha_i\beta(N_i^* - 2I_i^*) - t(2\beta I_i^* + gN_i^*) + k\beta I_j^* \\ &= \alpha_i\beta(N - 2I_i^*) - t(2\beta I_i^* + gN) + k\beta I_j^* \\ B_i &= k(\beta I_i^* + gN_i^*) \\ &= k(\beta I_i^* + gN) \\ C_{\alpha_1} &= \beta I_1^*(N_1^* - I_1^*) \\ &= \beta I_1^*(N - I_1^*) \end{aligned}$$

Recall that $\alpha_1 = m_1 abe^{-gn} = \frac{2\bar{\alpha}\bar{m}}{\bar{\alpha}+1} abe^{-gn}$.

This fact, along with equations (2)-(3), implies that

$$\frac{\partial I^*}{\partial \bar{\alpha}} = \frac{\partial \alpha_1}{\bar{\alpha}} \frac{\partial I^*}{\partial \alpha_1} = \frac{2\bar{m}abe^{-gn}}{(\bar{\alpha}+1)^2} \cdot \frac{C_{\alpha_1}(B_2 - A_2)}{A_1A_2 - B_1B_2}.$$

Proposition 5.0.1 in [1] states that $A_1A_2 - B_1B_2 > 0$, and the proof of this proposition states that $A_2 < 0$. Thus, $B_2 - A_2 > 0$ implies that $\frac{\partial I^*}{\partial \bar{\alpha}} > 0$. Recall that in the proof of the previous theorem, we showed that $\partial\bar{\alpha}/\partial V > 0$; consequently, I^* is an increasing function of the variance V.

□

References

1. Prosper O, Ruktanonchai N, Martcheva M (2012) Assessing the role of spatial heterogeneity and human movement in malaria dynamics and control. Journal of Theoretical Biology 303: 1–14.